Talanta 93 (2012) 264–273

Contents lists available at SciVerse ScienceDirect

Talanta

journal homepage: www.elsevier.com/locate/talanta

Probing cysteine self-assembled monolayers over gold nanoparticles – Towards selective electrochemical sensors

Ahmed Galal*, Nada F. Atta, Ekram H. El-Ads

Department of Chemistry, Faculty of Science, Cairo University, 12613 Giza, Egypt

ARTICLE INFO

Article history:
Received 9 August 2011
Received in revised form 11 February 2012
Accepted 15 February 2012
Available online 22 February 2012

Keywords:
Electrochemical sensor
Gold nanoparticles
Self-assembly monolayer
Neurotransmitters
Ascorbic acid

ABSTRACT

Cysteine forms self-assembled monolayers over gold nanoparticles. Based on this knowledge, a novel electrochemical sensor (Au-Au_{nano}-Cys-SDS) has been constructed by the formation of self-assembly monolayer (SAM) of cysteine on gold-nanoparticles modified gold electrode (Au-Au_{nano}-Cys) to be utilized for determination of dopamine in the presence of sodium dodecyl sulfate (SDS). Electrochemical investigation and characterization of the modified electrode sensor was achieved using cyclic voltammetry, electrochemical impedance spectroscopy, scanning electron, and atomic force microscopies. Au-Au_{nano}-Cys electrode in the presence of SDS gave comparable high current response to that of the gold nanoparticles modified gold electrode (Au-Au_{nano}). The Au-Au_{nano}-Cys-SDS electrode current signal was remarkably stable via repeated cycles and long term stability due to the strong Au—S bond. Very small peak separation, almost zero or 15 mV peak separation was also obtained by repeated cycles indicating unusual high reversibility. The oxidation peak current was determined to be linearly dependent on the dopamine concentration. A resulting calibration curve using square wave voltammetry (SWV) was obtained over concentration range of 30–100 $\mu mol\,L^{-1}$ and 120–320 $\mu mol\,L^{-1}$ with correlation coefficients of 0.996 and 0.994 and a limit of detection of 16 and 57 $nmol\,L^{-1}$, respectively. Using differential pulse voltammetry (DPV), a highly selective and simultaneous determination of tertiary mixture of ascorbic acid AA, dopamine, and acetaminophen APAP was explored at this modified electrode. It has been demonstrated that Au-Au_{nano}-Cys-SDS electrode can be used as a sensor with excellent reproducibility, sensitivity, and long term stability.

1. Introduction

Catecholamines are a class of neurotransmitters, and their detection in the human body has been of great interest to neuroscientists [1]. Dopamine (DA) is one of the most significant catecholamines and belongs to the family of excitatory chemical neurotransmitters. It plays a very important role in the functioning of the central nervous, cardiovascular, renal and hormonal systems, as well as a key role in drug addiction, and Parkinson's disease [2]. Tremendous consideration has been given in biomedical research; to design selective, sensitive and reliable methods for the direct measurement of dopamine in the presence of interfering molecules. Electrochemical analysis of binary or tertiary mixture on unmodified electrodes such as glassy carbon (GC), Pt, Au electrodes has limitations because of overlapping voltammetric peaks, fouling due to adsorption of byproducts and high detection limits [1–4]. To overcome these problems, various modified electrodes have been constructed. Some examples of modified electrodes include Pd and Pt nanoclusters modified poly(3-methylthiophene) (PMT), poly(N-methylpyrrole) (PMPy) and polyfuran film-coated platinum (Pt) electrode [1–4], poly(3,4-ethylene dioxythiophene) (PEDOT) modified Pt electrode in the presence of sodium dodecyl sulfate (SDS) [5], gold nanoparticles [6–12], self-assembled monolayer (SAM) [13–32], and gold nanoparticles immobilized on SAM modified electrodes [33–37]. Self-assembly procedure is precise modification of the surface structure in nanometer-scale, which was employed recently in surface protection, electronics, and fabrication of sensors and biosensors [18].

SAM which was formed by spontaneous adsorption of self-assembling molecules on metals such as gold, silver, copper, iron, nickel, or platinum [23,30,38,39], was found as an elegant way to orient as well as address electrically a molecular component of interest [23]. In particular the self-assembly of organosulfur compounds on gold surface has been extensively studied [19]. It has been shown that organosulfur compounds upon spontaneous chemisorption on gold surface, lose the hydrogen from the thiol group as molecular hydrogen H_2 [30] resulting in a strong, covalent and thermodynamically favored S—Au bond formation [21]. The reason for adsorbing thiols on gold as a preferred substrate is

* Corresponding author. Tel.: +20 0237825266; fax: +20 0235727556.
E-mail addresses: galal@sci.cu.edu.eg, galalh@sti.sci.eg, galalah1@yahoo.com (A. Galal).

0039-9140/$ – see front matter © 2012 Elsevier B.V. All rights reserved.
doi:10.1016/j.talanta.2012.02.032

based on two considerations: first, gold is a relatively inert metal and does not form stable oxides on its surface, second, it has a strong specific interaction with sulfur, which allows the formation of stable monolayers [30] in a very reproducible way [38] and in a short time [40]. The stable, well-organized, and densely packed [28] SAMs formed by thiols on gold electrodes offer advantages such as selectivity, sensitivity, short response time, and small overpotential in electrocatalytic reactions [18].

SAM utilizing 3-mercaptopropylphosphonic acid [13], 16-mercaptohexadecanoic acid [14], 4-mercaptopyridine [17], 4-amino-2-mercaptopyrimidine [19], thionine, thiolactic acid [21], homocysteine [22], 3-mercaptopropionic acid [16,27,41], mercaptoundecanoic acid [27], cysteamine [18,24,25,33], 6-mercaptonicotinic acid [26], and cysteine [40–55] modified gold electrodes were used for sensor and biosensor applications and immobilization of enzymes, proteins and DNA. Cysteine (Cys), a small thiol-containing amino acid, contains carboxyl, amino and thiol functionalities with respective pK_a values of 1.71, 8.33 and 10.78 [42] and is considered perfect in biochemical and electrochemical sensor research [54]. The side chain on cysteine is thiol, which is non-polar and thus cysteine is usually classified as a hydrophobic amino acid that allows this molecule to interact with different chemical species.

Gold nanoparticles have potential applications in the construction of electrochemical sensors and biosensors, where they function as "electron antennae" efficiently channeling electrons between the electrode and the electroactive species. This promotes better electron transfer between the electrode surface and the electrolyte due to their small dimensional size [8], good stability, biocompatibility [7,12], good conductivity and excellent catalytic activity [8,9]. On the other hand, gold nanoparticle modifications could largely increase the immobilized amount of S-functionalized compounds and enhance the Au—S bond and stability of SAMs layer [56]. Mercaptopropionic acid, gold nanoparticles and cystamine modified gold bare electrodes have been applied in voltammetric sensors for simultaneous detection of epinephrine (EP), ascorbic and uric (UA) acids [56].

Surfactants have been widely applied in electrochemistry to improve the property of the electrode/solution interface [5] in electroplating, corrosion, fuel cells, electrocatalysis, and electroanalysis [57,58]. In addition, they have proven effective in the electroanalysis of some biological compounds and drugs. In the presence of sodium dodecylbenzene sulfonate SDBS, gold nanoparticles modified glassy carbon electrodes exhibited good performance on the electrochemical oxidation of tryptophan [59]. Atta et al. fabricated a novel biosensor using poly(3,4-ethylene dioxythiophene) modified Pt electrode for selective determination of dopamine in presence of high concentrations of ascorbic acid and uric acid in the presence of sodium dodecyl sulfate (SDS). SDS forms a monolayer on polymer surface with a high density of negatively charged end directed outside the electrode. The electrochemical response of dopamine was improved by SDS due to the enhanced accumulation of protonated dopamine via electrostatic interactions. The common overlapped oxidation peaks of ascorbic acid, uric acid, and dopamine can be resolved by using SDS as the DA current signal increases while the corresponding signals for ascorbic acid and uric acid are quenched [5].

The aim of this work is to study the electrochemical behavior of selected neurotransmitters at solid electrodes modified with cysteine SAMs over gold nanoparticles. Extensive research has been devoted to self-assembly monolayer adsorption at gold electrodes. However, few publications have addressed SAMs of cysteine at nano-gold particles modified gold electrode. In addition, the resulting electrochemical behavior and determination of neurotransmitters in presence and absence of surfactants at this modified surface were not addressed.

2. Experimental

2.1. Chemicals and reagents

All chemicals were used without further purification. Dopamine (DA), ascorbic acid (AA), acetaminophen (APAP), hydroquinone (HQ), catechol (CA), epinephrine (E), norepinephrine (NE), 3,4-dihydroxy phenyl acetic acid (DOPAC), L-DOPA, potassium phosphate (mono, di-basic salt), cysteine (Cys), sodium dodecyl sulfate (SDS) and hydrogen tetrachloroaurate ($HAuCl_4$) were supplied by Aldrich Chem. Co. (Milwaukee, WI, USA). Aqueous solutions were prepared using double distilled water. Phosphate buffer solution PBS (1 mol L^{-1} K_2HPO_4 and 1 mol L^{-1} KH_2PO_4) of pH 2.58 was used as the supporting electrolyte.

2.2. Electrochemical cells and equipments

Electrochemical deposition and characterization were carried out with a three-electrode/one compartment glass cell. The working electrodes were gold, platinum and glassy carbon disc (diameter: 1 mm). The auxiliary electrode was in the form of 6.0 cm platinum wire. All potentials in the electrochemical studies were referenced to Ag/AgCl (4 mol L^{-1} KCl saturated with AgCl) electrode. Working electrodes were polished using alumina (2 μM)/water slurry until no visible scratches were observed. Prior to immersion in the cell, the electrode surface was thoroughly rinsed with distilled water and dried. All experiments were performed at 25 °C.

The gold nanoparticles electrosynthesis and their electrochemical characterization were performed using a BAS-100B electrochemical analyzer (Bioanalytical Systems, BAS, West Lafayette, USA). A Quanta FEG 250 instrument was used to obtain the scanning electron micrographs of the different films. The topographs of bare Au, Au-Au_{nano}, and Au-Au_{nano}-Cys-SDS electrodes were investigated with atomic force microscopy AFM (SPM, Shimadzu, Japan).

2.3. Electrodeposition of gold nanoparticles

The gold nanoparticles electrodeposition was achieved in a three-electrode/one compartment electrochemical cell with a solution containing 6 mmol L^{-1} $HAuCl_4$ and 0.1 mol L^{-1} KNO_3 (prepared in doubly distilled water and deaerated by bubbling with nitrogen). The potential applied between the working electrode (bare gold electrode) and the reference Ag/AgCl (4 mol L^{-1} KCl saturated with AgCl) electrode was held constant at −400 mV (Bulk electrolysis, BE) for 400 s [6]. The surface coverage of gold nanoparticles was 2.042×10^{-6} mol/cm^2 (estimated from the quantity of charge used in the electrodeposition process). This electrode is denoted as Au-Au_{nano}.

2.4. Different modification of the electrodes by cysteine

Self-assembly monolayer of cysteine was formed on bare electrodes (Au, GC and Pt) and gold nanoparticles modified gold electrode by soaking the electrode in 5 mmol L^{-1} cysteine/0.1 mol L^{-1} PBS (pH 2.58) for 5 min at room temperature. These electrodes are denoted as Au-Cys, GC-Cys, Pt-Cys, and Au-Au_{nano}-Cys, respectively. The modified electrodes were washed with doubly distilled water to remove the physically adsorbed species and dried carefully without touching the surface.

Other modifications are done by the successive additions of 10 μL of 0.1 mol L^{-1} SDS to the dopamine solution (1 mmol L^{-1} DA/0.1 mol L^{-1} PBS, pH 2.58) from 0 up to 160 μL and from 0 up to 40 μL in the case of Au-Au_{nano} and Au-Au_{nano}-Cys, respectively and the electrodes are denoted as Au-Au_{nano}-SDS and Au-Au_{nano}-Cys-SDS, respectively. After each addition, stirring

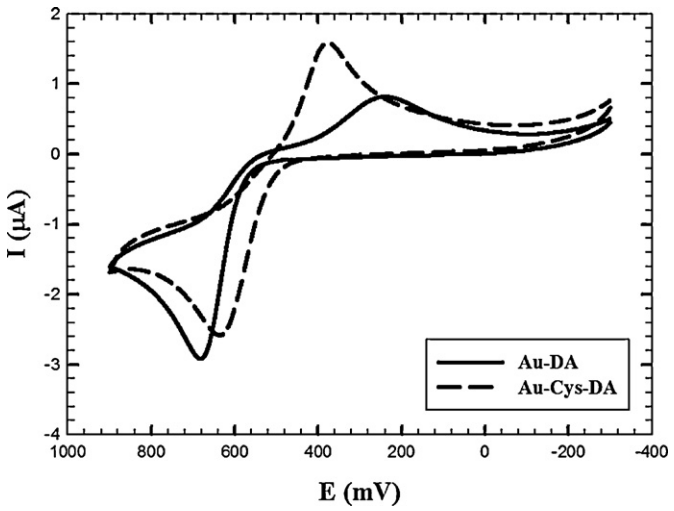

Fig. 1. CVs of 1 mmol L^{-1} DA/0.1 mol L^{-1} PBS (pH 2.58) at bare Au and Au-Cys electrodes, scan rate 50 mV s^{-1}.

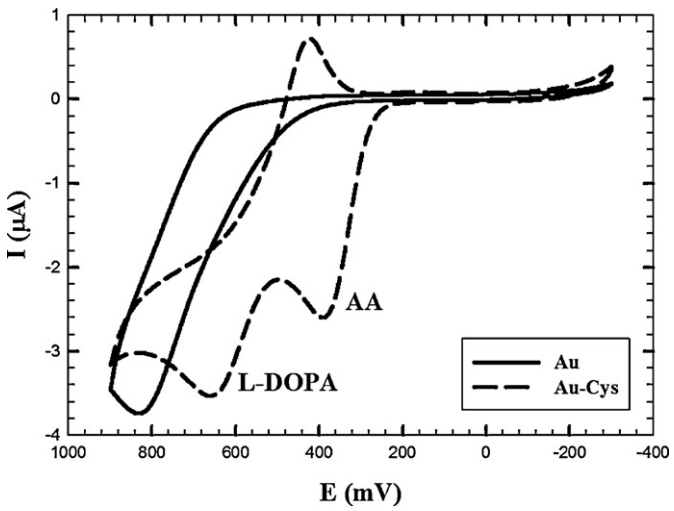

Fig. 2. CVs of separation of binary mixture of: 1 mmol L^{-1} AA and 1 mmol L^{-1} L-DOPA at bare Au and Au-Cys electrodes, scan rate 50 mV s^{-1}.

takes place for 5 min then holds for 1 min before running the experiment.

2.5. Electrochemical impedance spectroscopy (EIS)

EIS was performed using a Gamry-750 instrument and a lock-in-amplifier that was connected to a personal computer. The data analysis was provided with the instrument and applied non-linear least square fitting with Levenberg–Marquardt algorithm. All impedance experiments were recorded between 0.1 Hz and 100 kHz with an excitation signal of 10 mV amplitude. The measurements were performed under potentiostatic control at different applied potentials which were decided from the cyclic voltammograms recorded for the modified electrodes.

3. Results and discussion

3.1. Electrochemistry of DA at cysteine modified gold electrode

Fig. 1 shows the cyclic voltammetric (CV) behavior of 1 mmol L^{-1} DA in 0.1 mol L^{-1} PBS (pH 2.58) tested at bare gold electrode Au (solid line) and gold modified with cysteine Au-Cys (dash line). It is clear that the redox voltammetric peaks of DA at bare gold electrode is quasi-reversible with peak potential separation (ΔE_p = 448 mV), suggesting slow electron transfer kinetics, presumably due to the fouling of the electrode surface by the oxidation products. However, a relatively well-defined redox waves with better reversibility of DA were obtained at Au-Cys electrode. The oxidation peak potential shifts negatively to 636 mV, and the reduction peak potential shifts positively to 379 mV (ΔE_p = 257 mV). The reduction peak current increases significantly from 0.48 μA to 2.1 μA at Au-Cys electrode as compared to the bare Au electrode. The Au-Cys SAM modified electrode affects the mechanistic redox reaction of DA with two types of interactions. The first is the interaction between Au and cysteine through thiol group of cysteine to form strong covalent Au—S bond (molecule–substrate interaction). The second interaction is between cysteine on Au and DA molecules through amino group of cysteine and hydroxyl-phenol group of DA via hydrogen bond formation (molecule–molecule interaction). The DA on Au-Cys electrocatalytic oxidation is due to the formation of a hydrogen bond between hydroxyl-phenol of DA and the nitrogen in the Cys-SAM. The hydrogen bond formation has a great impact on the activation of the hydroxyl-phenol on the benzene ring. As a result, the bond energy between hydrogen and oxygen is weakened and the electron transfer is more likely to occur via N···H—O bond. Thus, the Cys-SAM system can act as a promoter to increase the rate of electron transfer, lowering the overpotential of DA at the modified electrode, and enhancing the reversibility of the redox reaction of dopamine.

Also, Au-Cys electrode shows excellent stability via repeated cycles (Supplement 1) which means no fouling of surface by oxidized products of DA as seem on bare gold electrodes. Thus Au-Cys electrode is a chemically modified electrode demonstrates antifouling properties with excellent stability for the oxidation of neurotransmitters. The same study was done for other compounds such as E, NE, DOPAC, L-DOPA, HQ, CA, and AA and the trend was repeated.

3.2. Binary and tertiary mixture separation at cysteine SAM modified gold electrode

Fig. 2 shows CVs for the analysis of a binary mixture of 1 mmol L^{-1} AA, and 1 mmol L^{-1} L-DOPA in 0.1 mol L^{-1} PBS (pH 2.58) at bare Au (solid line) and Au-Cys (dash line) electrodes. An unresolved oxidation peak at 833 mV was observed illustrating that the oxidation peaks of AA, and L-DOPA cannot be separated on the bare Au electrode. However, two resolved peaks were obtained at Au-Cys electrode at 391 mV and 659 mV for AA and L-DOPA, respectively. This indicates that this sensor can be used for the simultaneous determination of AA and L-DOPA. Also, the analysis of a binary mixture of 1 mmol L^{-1} AA, and 1 mmol L^{-1} DA in 0.1 mol L^{-1} PBS (pH 2.58) at bare Au electrode and Au-Cys modified electrode was studied and two well separated signals were obtained at Au-Cys electrode at 402 mV, and 606 mV for AA, and DA, respectively (figure not shown). In addition, Au-Cys electrode can be used to separate tertiary mixture of 1 mmol L^{-1} AA, 1 mmol L^{-1} DA, and 1 mmol L^{-1} APAP in 0.1 mol L^{-1} PBS (pH 2.58) as evidenced by three resolved peaks at 356 mV, 556 mV, and 664 mV for AA, DA, and APAP, respectively (Supplement 2).

3.3. The effect of cysteine SAM on different substrates

Cysteine SAM was formed by spontaneous adsorption of self-assembled molecules on metals such as gold, silver, copper, iron, nickel, palladium or platinum [23,30,38,60]. Fig. 3(A) shows the CVs of 1 mmol L^{-1} DA in 0.1 mol L^{-1} PBS (pH 2.58) at different electrodes (Au, Pt, and GC) modified with cysteine. If we compare these CVs with those obtained at bare electrodes, we concluded

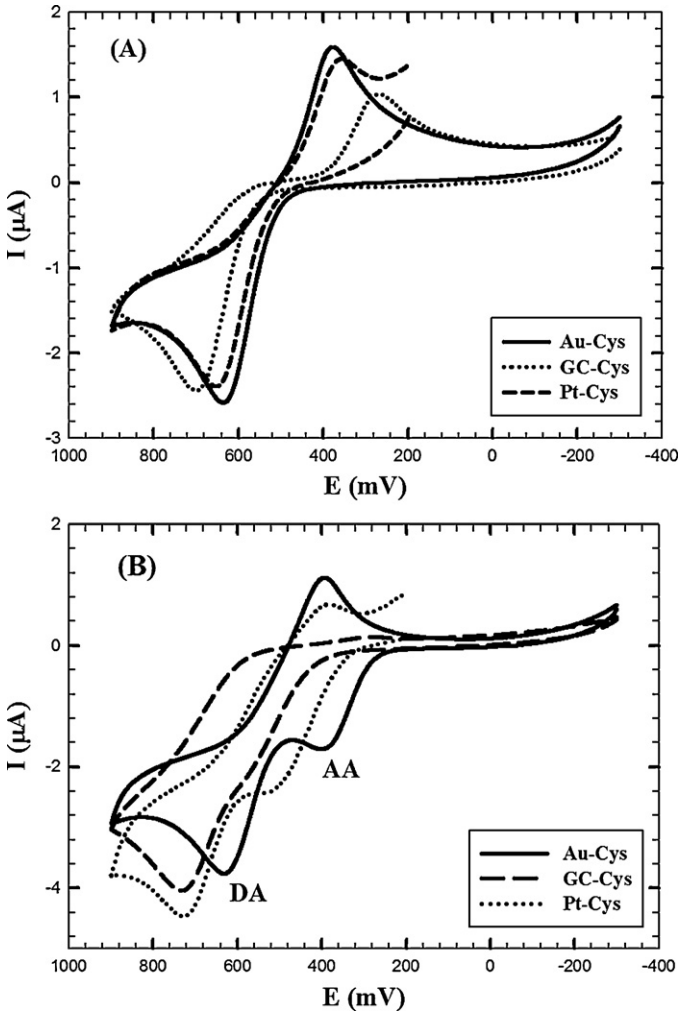

Fig. 3. (A) CVs of 1 mmol L^{-1} DA at Au-Cys, Pt-Cys, and GC-Cys electrodes, (B) CVs of binary mixture of 1 mmol L^{-1} AA and 1 mmol L^{-1} DA at Au-Cys, GC-Cys, and Pt-Cys electrodes, scan rate 50 mV s^{-1}.

the effect of cysteine as a promoter of electron transfer and as a bridge molecule is more pronounced on Au substrate. This is due to the strong affinity of gold to thiol compounds and formation of strong, stable, covalent, and thermodynamically favored Au—S bonds. Also, observes was the partial interaction between the Pt electrode and cysteine molecules which shifted the oxidation peak of DA from 680 mV at bare Pt to 653 mV at Pt-Cys with the reduction peak appearing at 356 mV at Pt-Cys electrode. The effect of cysteine on GC electrode is less pronounced with the oxidation peak and reduction peak of DA shifting from 738 mV, and 236 mV at bare GC electrode to 700 mV and 269 mV at GC-Cys electrode, respectively.

Fig. 3(B) shows the cyclic voltammograms of the separation of binary mixture of 1 mmol L^{-1} AA, and 1 mmol L^{-1} DA in 0.1 mol L^{-1} PBS (pH 2.58) at Au-Cys (solid line), GC-Cys (dash line), and Pt-Cys (dotted line) modified electrodes. Two well-separated oxidation peaks were obtained using Au-Cys electrode at 402 mV and 606 mV for AA, and DA, respectively. However, an overlapped combined oxidation peak is obtained at GC-Cys electrode at 731 mV. At Pt-Cys electrode, the two oxidation peaks are more resolved and separated than at GC-Cys electrode and this ensures the partial interaction between cysteine and Pt electrode. These results ensure the strong effect of cysteine on gold electrode.

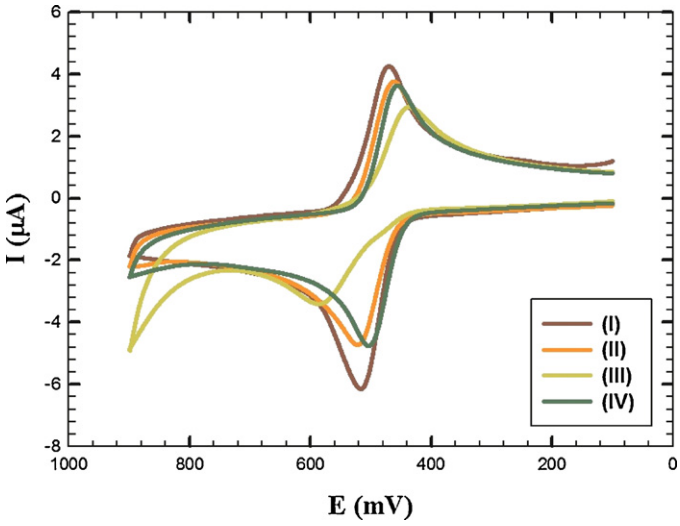

Fig. 4. CVs of 1 mmol L^{-1} DA at: (I) Au-Au_{nano}, (II) Au-Au_{nano}-SDS, (III) Au-Au_{nano}-Cys, and (IV) Au-Au_{nano}-Cys-SDS modified electrodes, scan rate 50 mV s^{-1}.

3.4. Electrochemistry of dopamine at different modified electrodes in presence of SDS

Fig. 4 shows the electrochemistry of DA at different modified electrodes (Au-Au_{nano}, Au-Au_{nano}-SDS, Au-Au_{nano}-Cys, and Au-Au_{nano}-Cys-SDS). Fig. 4(I) shows the electrochemistry of DA at gold nanoparticles modified Au electrode (Au-Au_{nano}). A remarkable increase in the current response (I_{pa} = 5.6 μA) was observed, followed by a drop in the oxidation peak potential (E_{pa} = 516 mV), and enhancement in the reversibility (ΔE_p = 45 mV). These observations are due to the catalytic effect of gold nanoparticles acting as a promoter to enhance the electrochemical reaction, thereby, considerably accelerating the rate of electron transfer [6]. Fig. 4(II) shows the CV response of DA at gold nanoparticles modified electrode in presence of SDS (160 μL). The successive additions of 10 μL of 0.1 mol L^{-1} SDS to 1 mmol L^{-1} DA leads to decreasing the oxidation current of DA from 5.6 μA in absence of SDS to 4.2 μA in presence of 160 μL of SDS (increments add 6.7×10^{-5} mol L^{-1} SDS of each addition and the total concentration of SDS after 16 additions is 1.1×10^{-3} mol L^{-1}). This indicates there is an interaction between gold nanoparticles and SDS which leads to decreasing oxidation current of DA. SDS is an anionic surfactant with a hydrophobic tail consisting of 12 carbon atoms and a hydrophilic head containing sulfate group. SDS interacts with gold nanoparticles through its hydrophobic carbon chain, blocking the binding sites on gold nanoparticles and acting as an insulating layer rather than enhancing the charge transfer [57,58]. Thus, the oxidation current of DA decreases in presence of SDS.

Fig. 4(III) shows the CV of DA at cysteine SAM modified gold nanoparticles (Au-Au_{nano}-Cys). The presence of cysteine SAM on gold nanoparticles leads to decreasing the oxidation peak current of DA from 5.6 μA to 3 μA, shifting the oxidation potential from 516 mV to 586 mV, and increasing the peak separation from 45 mV to 148 mV. This is due to the following: (a) the disorganization of cysteine molecules on gold nanoparticles which inhibits the formation of hydrogen bond between DA and cysteine; and (b) electrostatic repulsion between the positively charged cysteine and positively charged DA which hinders DA from reaching the electrode surface. Fig. 4(IV) shows the CV of DA at cysteine SAM modified gold nanoparticles in presence of SDS (Au-Au_{nano}-Cys-SDS). The successive additions of 10 μL of 0.1 mol L^{-1} SDS up to 40 μL (increments add 6.7×10^{-5} mol L^{-1} SDS of each addition and the total concentration of SDS after four additions is

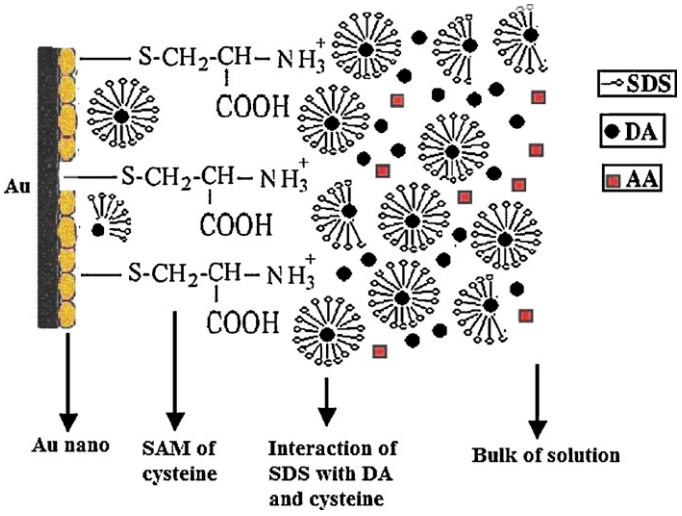

Scheme 1. Schematic model of Au-Au_{nano}-Cys-SDS electrode in presence of DA cation and AA.

2.7×10^{-4} mol L^{-1}) leads to increasing the oxidation current from 3 μA to 4.3 μA, shifting the oxidation potential from 586 mV to 504 mV and decreasing the peak separation from 148 mV to 47 mV in presence of 40 μL SDS. The schematic model of Au-Au_{nano}-Cys-SDS electrode is illustrated in Scheme 1. There is an electrostatic attraction between the cationic DA and the anionic SDS which enhances the diffusion of DA through the positively charged cysteine SAM. Also there is an interaction between the positively charged cysteine and anionic SDS which allows the reorganization of cysteine molecules on gold nanoparticles. This enhances the hydrogen bond formation between DA and cysteine and promotes faster electron transfer kinetics.

When the CVs of DA at Au-Cys and Au-Au_{nano}-Cys electrodes are compared, it is concluded that the effect of cysteine on the response of polycrystalline bare Au is more pronounced than that on gold nanoparticles. The effect of adding SDS on gold nanoparticles results in enhanced signal response. This allows the reorganization of cysteine on gold nanoparticles that results in the increase of the oxidation current, decrease in the peak separation and hence better reversibility.

Au-Au_{nano} electrode displays a little higher current response but Au-Au_{nano}-Cys in presence of SDS gives beside high current response, shows better repeatability and long term stability. This study will focus on Au-Au_{nano}-Cys-SDS electrode.

3.5. Stability of the modified electrodes

The stability of the different modified electrodes was studied via repeated cycles up to 50 cycles. Au-Au_{nano}, Au-Au_{nano}-SDS (160 μL), Au-Au_{nano}-Cys, and Au-Au_{nano}-Cys-SDS (40 μL) electrodes in 1 mmol L^{-1} DA/0.1 mol L^{-1} PBS (pH 2.58) produced excellent stability as evidenced by noticeable decrease in current response indicating that these modified electrodes have a good reproducibility and do not suffer from surface fouling during the repetitive voltammetric measurement [5]. In comparison, the bare Au electrode demonstrated poor stability relative to the modified electrodes due to surface fouling by cysteine oxidation products.

Very small peak separation (almost zero or 15 mV peak separation) was obtained indicating unusually high reversibility through repeated cycling (Supplement 3). Comparing the stability of the CVs for the 1st, 25th, and 50th cycles on the Au-Au_{nano}-Cys electrode (figure not shown), it was observed that I_{pa} increased from 2.5 μA in the 1st cycle up to 3.8 μA in the 25th and 50th cycles. Also, the peak separation decreased from 120 mV in the 1st cycle to ~0 mV in the 25th and 50th cycles. This indicates that cysteine molecules are reorganized on gold nanoparticles by repeated cycles. This reorganization enhances the hydrogen bond formation between DA and cysteine which increases the electron transfer rate. Thus, cysteine molecules are reorganized on gold nanoparticles by repeated cycles or by the addition of SDS (instantaneous reorganization).

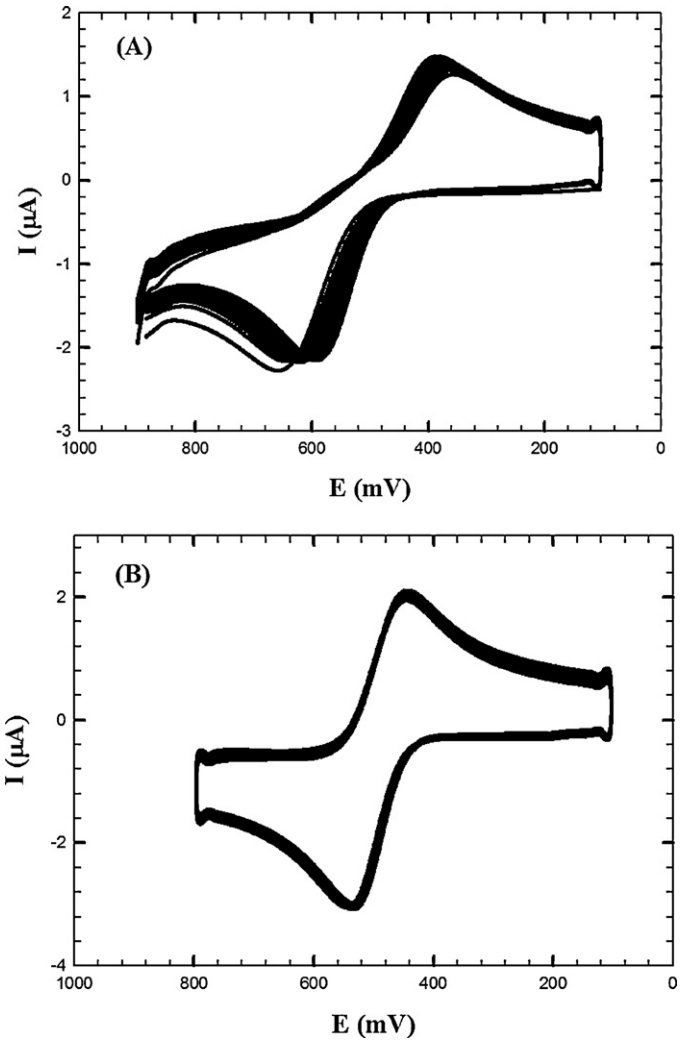

Fig. 5. Long term stability of: (A) Au-Au_{nano} and (B) Au-Au_{nano}-Cys-SDS (40 μL) after one week, 50 repeated cycles, 50 mV s^{-1} scan rate.

In addition, the long term stability of Au-Au_{nano}, Au-Au_{nano}-Cys and Au-Au_{nano}-Cys-SDS electrodes was studied for a time period of up to one week. After each measurement, the electrode was stored in 0.1 mol L^{-1} PBS (pH 2.58) in the refrigerator (at 5 °C). Fig. 5(A) and (B) shows the repeated cycles after one week of storage of Au-Au_{nano}, and Au-Au_{nano}-Cys-SDS electrodes, respectively. In the case of Au-Au_{nano} electrode, I_{pa} of the 50th cycle decreased by 26%, and 44% after 3 days and 1 week, respectively. Peak separation increased to 120 mV, and 180 mV after 3 days and one week of storage, respectively.

In the case of Au-Au_{nano}-Cys electrode, I_{pa} of the 50th cycle decreased by 23.6%, and 35.6% after 3 days and 1 week, respectively. Peak separation was zero and 15 mV after 3 days and 1 week, respectively. Also, for Au-Au_{nano}-Cys-SDS electrode, I_{pa} decreased by 24% and the peak separation was 15, and 60 mV after 3 days and one week of storage, respectively. These results indicate that the presence of SAM of cysteine on gold nanoparticles enhances the reversibility and the long term stability of Au-Au_{nano}-Cys and

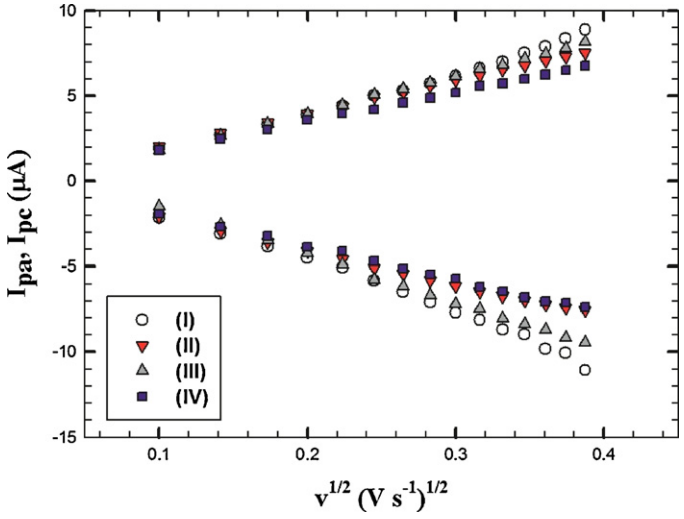

Fig. 6. Linear relationship of I_p vs. $\nu^{1/2}$ for 1 mmol L^{-1} DA at (I) Au-Au_{nano}, (II) Au-Au_{nano}-SDS, (III) Au-Au_{nano}-Cys, and (IV) Au-Au_{nano}-Cys-SDS.

Table 1
Values of diffusion coefficient of different modified electrodes.

Electrode type	D_{ox} ($cm^2\ s^{-1}$)	D_{red} ($cm^2\ s^{-1}$)
Bare Au	5.89×10^{-6}	6.97×10^{-8}
Au-Cys	3.66×10^{-6}	2.79×10^{-6}
Au-Au_{nano}	1.74×10^{-5}	1.16×10^{-5}
Au-Au_{nano}-Cys	5.00×10^{-6}	5.88×10^{-6}
Au-Au_{nano}-SDS	9.88×10^{-6}	1.01×10^{-5}
Au-Au_{nano}-Cys-SDS (40 μL)	1.06×10^{-5}	8.92×10^{-6}

Au-Au_{nano}-Cys-SDS electrodes due to the formation of strong Au—S bond.

3.6. Apparent diffusion coefficients

The diffusion coefficients of 1 mmol L^{-1} DA in 0.1 mol L^{-1} PBS (pH 2.58) at different modified electrodes have been calculated. The relation between anodic peak current (I_{pa} A) and the diffusion coefficient of the electroactive species (D $cm^2\ s^{-1}$), is given by Randles–Sevcik equation:

$$I_{pa} = (2.69 \times 105)n^{3/2}AC^{\circ}D^{1/2}\nu^{1/2}$$

where n is the number of electrons exchanged in oxidation at T = 298 K, A is the geometrical electrode area = 7.854×10^{-3} cm^2, C° is the analyte concentration (1×10^{-6} mol cm^{-3}) and v is the scan rate V s^{-1} [6]. It is important to note the apparent surface area used in the calculations does not take into account the surface roughness of gold nanoparticles (the roughness factor of bare gold and gold nanoparticles calculated from atomic force microscopy measurements are 0.656 and 1.07, respectively).

For a diffusion-controlled process, a plot of the anodic peak current values versus the square root of the scan rate results in a straight-line relationship. Fig. 6 shows a comparison of these linear relationships for DA at different modified electrodes: (I) Au-Au_{nano}, (II) Au-Au_{nano}-SDS, (III) Au-Au_{nano}-Cys and (IV) Au-Au_{nano}-Cys-SDS. Also, Table 1 summarizes the D_{app} values for DA at different modified electrodes. From Table 1 it is shown that the D_{app} values increase in the following order: Au-Au_{nano}-Cys < Au-Au_{nano}-SDS < Au-Au_{nano}-Cys-SDS < Au-Au_{nano}. These results confirm the previous results that the presence of cysteine SAM on bare Au electrode enhances the electron transfer rate. The sequence of increasing D_{app} obtained from scan rate effect is comparable with that obtained from chronoamperometry study.

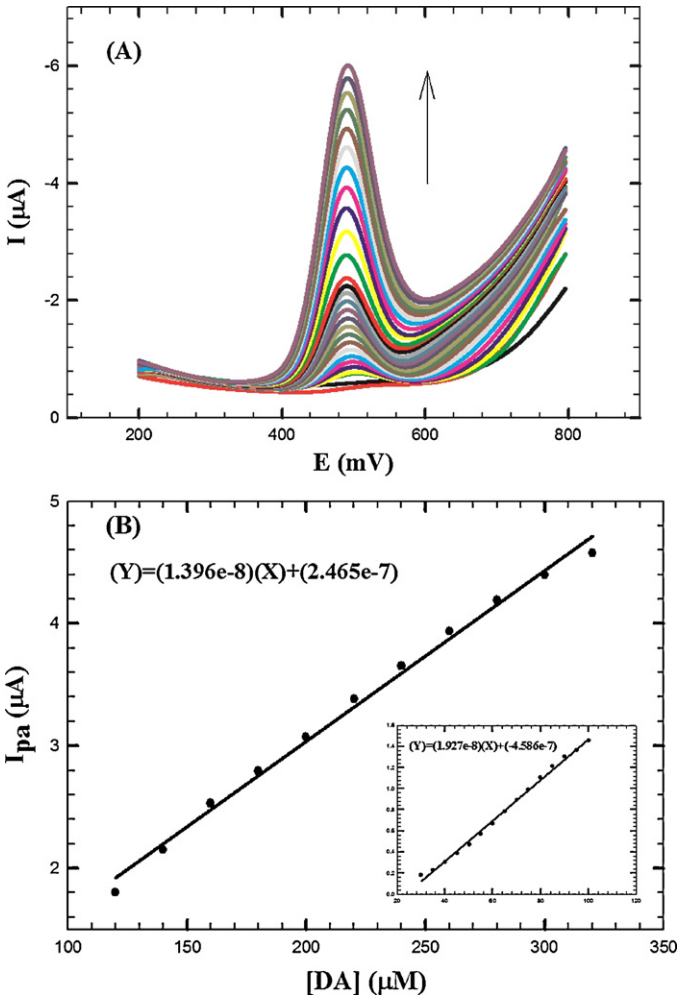

Fig. 7. (A) SWV of 15 mL of 0.1 mol L^{-1} PBS (pH 2.58) at Au-Au_{nano}-Cys electrode in presence of 40 μL of 0.1 mol L^{-1} SDS in different concentrations of DA (30–320 μmol L^{-1}), (B) calibration curve for DA of concentrations from (120 μmol L^{-1} to 320 μmol L^{-1}) and from (30 μmol L^{-1} to 100 μmol L^{-1}, the inset).

3.7. Determination of dopamine using Au-Au_{nano}-Cys in presence of SDS

The voltammetric behavior of DA was examined using square wave voltammetry (SWV). Fig. 7(A) shows typical SWV of successive additions of 10 μl of 1 mmol L^{-1} dopamine to 40 μL of 0.1 mol L^{-1} SDS in 15 mL of 0.1 mol L^{-1} PBS (pH 2.58) with the total concentration of SDS after 4 additions being 2.7×10^{-4} mol L^{-1}. Fig. 7(A) shows that by increasing the concentration of DA, the anodic peak current increased indicating the electrochemical response of DA is apparently improved by SDS addition due to enhanced accumulation of protonated DA via electrostatic interaction with negatively charged SDS at the Au-Au_{nano}-Cys electrode surface. Fig. 7(B) and the inset show the calibration curves of the anodic peak current values in the linear range of 30–100 μmol L^{-1} with the regression equation of I_p (A) = $1.927 \times 10^{-8}c$ (μmol L^{-1}) + (-4.586×10^{-7}) and 120–320 μmol L^{-1} DA with the regression equation of I_p (A) = $1.396 \times 10^{-8}c$ (μmol L^{-1}) + (2.465×10^{-7}) with correlation coefficients of 0.996 and 0.994 and detection limits of 16 nmol L^{-1} and 57 nmol L^{-1}, respectively. The detection limit was calculated from the equation:

$$\mathrm{DL} = \frac{3s}{b},$$

Table 2
Comparison for determination of dopamine at various modified electrodes based in literature reports.

Electrode	Compound	pH	LDR (μM)	Sensitivity (μA/μM)	LOD (nM)	Reference
CPE-Au_{nano}	DA	7.4	0.1–6	0.288	5.9	[6]
GC-CA-Au_{nano}	DA	7.0	0.01–25	9.79	4	[7]
ITO-Au_{nano}	DA	7.2	0.001–500	NR	0.53.0	[8]
	5-HT		0.01–250	NR		
Au-MPPA	DA in presence of 1 mM AA	7.4	0.4–20	0.0475	150	[13]
Au-Cys	UA	7.0	54–150	0.0099	2000	[53]
	AA		140–500	0.0040	11,000	
Au-Cys	HQ	4.8	2–200	0.034	400	[40]
Au-CA-Au_{nano}	DA in presence of 0.1 mM AA	7.2	NR	NR	220	[33]
Pt-PEDOT-SDS	DA	7.4	0.5–25	NR	61	[5]
Au-Au_{nano}-Cys-SDS	DA	2.58	30–100	0.0193	16	This work

LDR, linear dynamic range; LOD, limit of detection; NR, not reported; CPE, carbon paste electrode; CA, cysteamine; ITO, indium tin oxide; 5-HT, Serotonin; MPPA, 3-mercaptopropylphosphonic acid; HQ, hydroquinone.

where *s* is the standard deviation and *b* is the slope of the calibration curve. Table 2 shows the comparison for the determination of dopamine at Au-Au_{nano}-Cys-SDS electrode with various modified electrodes based in literature reports.

3.8. Effect of solution pH

It is known that buffer solution pH affects protonation of the amino acid and the sensitivity of the electrode. The effect of changing pH of the supporting electrolyte on the electrochemical response of DA was studied. Fig. 8 shows the CVs of 1 mmol L^{-1} DA in 0.1 mol L^{-1} PBS of pH 2.58, 7.00, and 9.00 at Au-Au_{nano}-Cys electrode in presence of 40 μL of 0.1 mol L^{-1} SDS with the total concentration of SDS after 4 additions being 2.7×10^{-4} mol L^{-1}. It should be mentioned that cysteine solution was prepared in 0.1 mol L^{-1} PBS of the same pH of the DA solution studied (2.58, 7.00, and 9.00) and SDS was prepared in double distilled water. It is evident that changing pH of the supporting electrolyte altered both peak potentials and the peak currents of dopamine. In general, all the oxidation and reduction peak potentials of DA shifted to less positive values upon using PBS of pH 7.00, and 9.00 as supporting electrolytes when compared to PBS of pH 2.58. The potential peaks separation were 47, 133, and 72 mV and the oxidation peak currents were 4.34, 2.7, and 5.13 upon using PBS of pH 2.58, 7.00, and 9.00, respectively. These results indicated that the electrocatalytic oxidation of DA at Au-Au_{nano}-Cys electrode in presence of 40 μL of 0.1 mol L^{-1} SDS is a pH-dependent reaction and protonation/deprotonation was taking part in the charge transfer process [58].

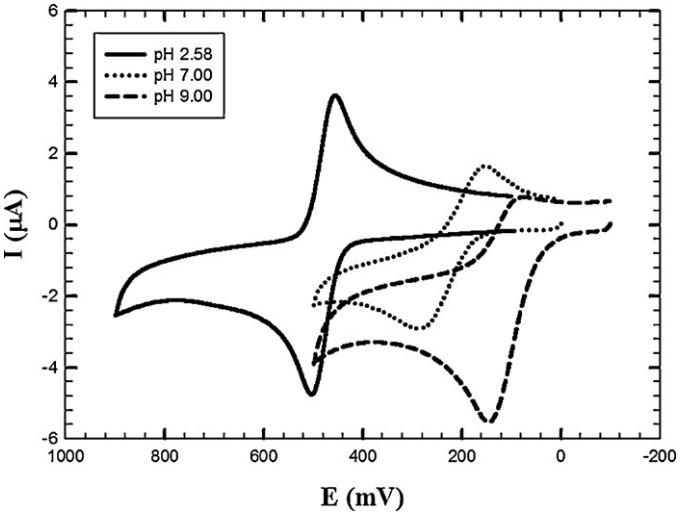

Fig. 8. CVs of 1 mmol L^{-1} DA in 0.1 mol L^{-1} PBS of different pH 2.58, 7.00, and 9.00 at Au-Au_{nano}-Cys electrode in presence of 40 μL of 0.1 mol L^{-1} SDS (increments add 6.7×10^{-5} mol L^{-1} SDS of each addition and the total concentration of SDS after 4 additions is 2.7×10^{-4} mol L^{-1}).

3.9. Electrochemical impedance spectroscopy (EIS) studies

EIS is regarded as an effective method to monitor the interfacial properties of surface-modified electrodes [5,6]. Therefore, EIS was used to investigate the nature of DA interaction at Au-Au_{nano}-Cys-SDS surface. EIS data were obtained for the modified electrode at ac frequency varying between 0.1 Hz and 100 kHz with an applied potential (510 mV) in the region corresponding to the electrolytic oxidation of DA in 0.1 mol L^{-1} PBS (pH 2.58).

Fig. 9(A) shows a typical impedance spectrum presented in the form of Nyquist plot of DA at Au-Au_{nano}-Cys-SDS electrode and the inset shows the typical impedance spectrum presented in the form of Bode plot. The experimental data were compared to an equivalent circuit that used some of the conventional circuit elements, namely; resistance, capacitance, diffusion, and induction elements [4,6]. The equivalent circuit is shown in Fig. 9(B). In this circuit, R_s is the solution resistance, RL1 is the resistance due to the surfactant film on the surface, RL2 is the resistance due to the SAM of cysteine, and R_{ct} is the charge transfer resistance. Capacitors in EIS experiments do not behave ideally; instead they act like a constant phase element (CPE) [4]. Therefore, CPE1 is a constant phase element and *n*1 is its corresponding exponent (*n* is less than one). Cc2 and Cc3 represent the capacitance of the double layer. Diffusion can create an impedance known as the Warburg impedance *Z*. Table 3 lists the best fitting values calculated from the equivalent circuit (Fig. 9(B)) for the impedance data of Fig. 9(A).

As shown in Fig. 9(A), the impedance spectra include a semicircle portion and a linear portion; the semicircle part at the higher frequencies corresponds to the electron-transfer limiting electrochemical process, and the linear part at the lower frequencies

Table 3
EIS fitting data corresponding to Fig. 9(A).

RL1/ 10^4 Ω cm^2	RL2/ Ω cm^2	R_{ct}/ 10^3 Ω cm^2	Cc3/ 10^{-5} F cm^{-2}	R_s/ 10^2 Ω cm^2	Cc2/ 10^{-8} F cm^{-2}	CPE1/ 10^5 F cm^{-2}	*n*1	*Z* 10^4 Ω $s^{-1/2}$
5.268	31.06	2.294	3.603	4.838	8.201	3.191	0.9094	1.926

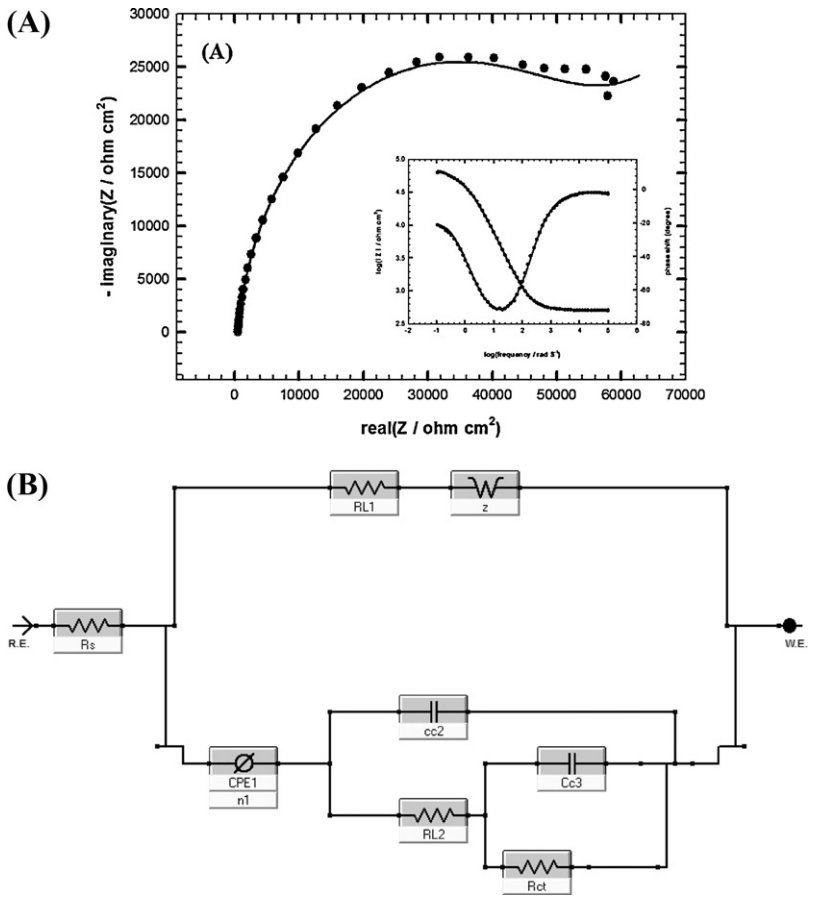

Fig. 9. (A) Nyquist plot of Au-Au_{nano}-Cys-SDS electrode in 1 mmol L^{-1} DA/0.1 mol L^{-1} PBS (pH 2.58) at the oxidation potential (510 mV), and the inset, the typical impedance spectrum presented in the form of Bode plot (symbols and solid lines represent the experimental measurements and the computer fitting of impedance spectra, respectively), frequency range: 0.1–100,000 Hz. (B) The equivalent circuit used in the fit procedure of the impedance spectra.

corresponds to the diffusion-limiting electrochemical process. The semicircle diameter equals the interfacial charge transfer resistance R_{ct}. This resistance controls the electron transfer kinetics of the redox probe at the electrode interface. Therefore, R_{ct} can be used to describe the interface properties of the electrode [6]. The semicircle part in Fig. 9(A) is relatively small, implying a low charge transfer resistance R_{ct} of the redox probe and this indicates the conductivity of the modified electrode and the facilitation of charge transfer. The values of the capacitive component indicate the conducting character of the modified surface due to ionic adsorption at the electrode surface and the charge transfer process.

3.10. Analysis of tertiary mixture at Au-Au_{nano}-Cys-SDS

The determination of catecholamines in biological samples is crucial for the diagnosis of many diseases. However, electrochemical oxidation of catecholamines especially DA at conventional electrodes is found difficult because of interference due to the co-existence of interfering compounds such as ascorbic acid (AA) and others in the biological fluids, which also undergo oxidation more or less at the same potential. Acetaminophen (paracetamol), APAP, is also likely to interfere with DA and AA determination [4]. Fig. 10 shows the differential pulse voltammogram of tertiary mixture of 1 mmol L^{-1} AA, 1 mmol L^{-1} DA and, 1 mmol L^{-1} APAP in 0.1 mol L^{-1} PBS (pH 2.58) at Au-Au_{nano}-Cys with successive additions of 0–40 μL of 0.1 mol L^{-1} SDS. The inset of Fig. 10 shows the DPVs of the mixture in the absence of SDS and presence of SDS. Three well-defined oxidation peaks were obtained at Au-Au_{nano}-Cys electrode at 300, 468, and 648 mV for AA, DA,

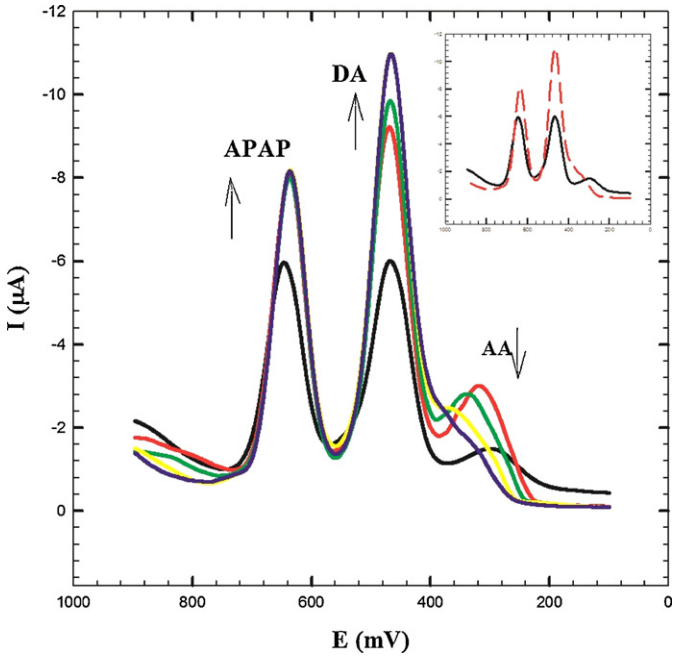

Fig. 10. Differential pulse voltammogram for 1 mmol L^{-1} AA, 1 mmol L^{-1} DA and 1 mmol L^{-1} APAP in PBS (0.1 mol L^{-1}), at Au-Au_{nano}-Cys with successive additions of (0–40 μL) 0.1 mol L^{-1} SDS, at pH 2.58, inset represents the initial (in absence of SDS) and final (in presence of 40 μL SDS) DPVs.

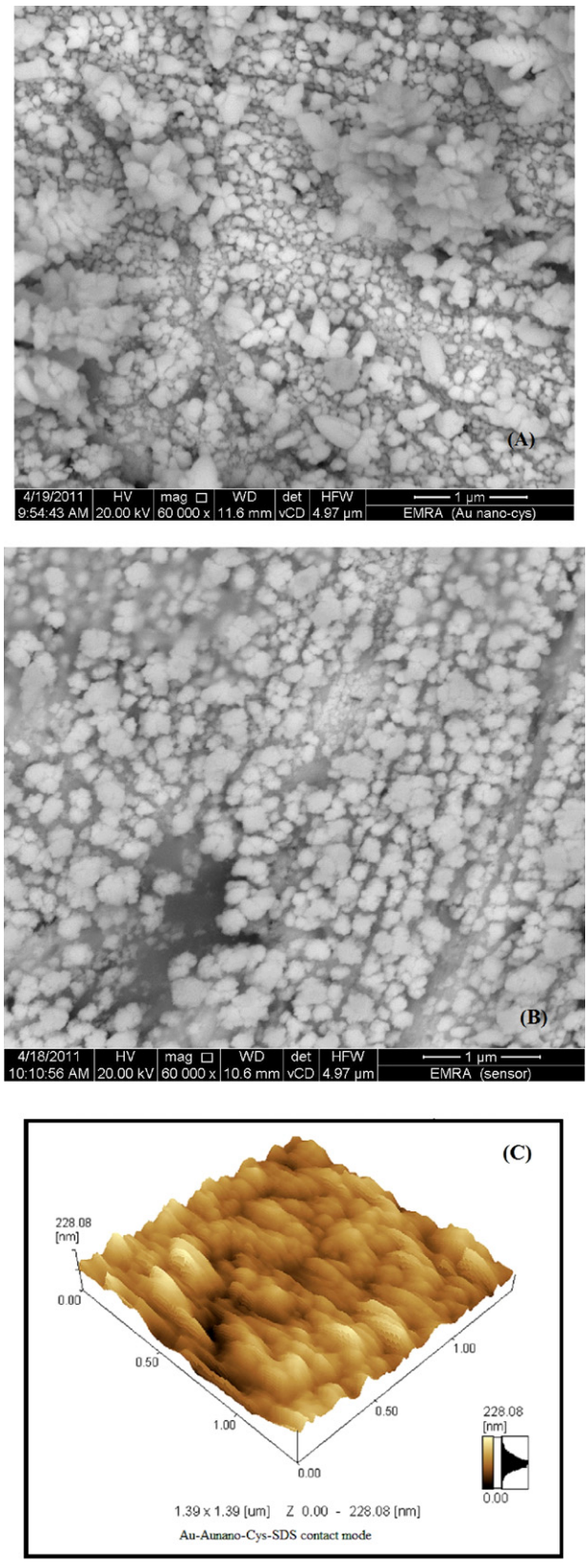

Fig. 11. SEM images of: Au-Au_{nano}-Cys (A), Au-Au_{nano}-Cys-SDS (B) electrodes, and AFM image by contact mode of Au-Au_{nano}-Cys-SDS electrode (C).

and APAP, respectively. Thus Au-Au_{nano}-Cys electrode can be used for the simultaneous determination of AA, DA, and APAP in a mixture. By the successive additions of 10 μL of 0.1 mol L^{-1} SDS in the mixture solution, the oxidation peak current of DA and APAP increases while the oxidation current of AA decreases until eventual complete disappearance. It is expected that the addition of SDS will cause a formation of a surfactant film over Au-Au_{nano}-Cys electrode. This amiphilic film will align in a way where the head groups of surfactant molecules face the aqueous medium leaving the hydrophobic part in contact with each other and away from the aqueous medium. The negative charge of the adsorbed surfactant film as well as the hydrophobic character of the interior of this film will act to repel hydrophilic AA molecules or its AA^- away from the electrode surface while enhancing the preconcentration/accumulation of hydrophobic cations of DA and APAP. This concept is illustrated in Scheme 1 [5]. Au-Au_{nano}-Cys electrode stability for mixture separation in presence of SDS was studied via repeated cycling up to 50 cycles with excellent stability being demonstrated (Supplement 4). Also, long term stability for separation of tertiary mixture of AA, DA, and APAP on Au-Au_{nano}-Cys electrode was studied in presence of SDS. After 3 days and one week of storage, I_{pa} of DA decreased by 14% and 17% and I_{pa} of APAP decreased by 15% and 28%, respectively. In addition, the long term stability for the separation of the same mixture at Au-Au_{nano} electrode was studied. After 3 days and one week of storage, I_{pa} of DA decreased by 34% and 44% and I_{pa} of APAP decreased by 9% and 33%, respectively. Thus, Au-Au_{nano}-Cys in presence of SDS gives better stability via repeated cycles and longer term stability not only for DA detection, but also for tertiary mixture separation.

3.11. Surface morphology of Au-Au_{nano}-Cys-SDS electrode

The response of an electrochemical sensor was related to the physical morphology of its surface. Several factors such as surface roughness, porosity of films, and inclusion of defects should affect the current response of the electrode. The SEM images of Au-Au_{nano}-Cys and Au-Au_{nano}-Cys-SDS electrodes are shown in Fig. 11(A) and (B), respectively. As observed in the SEM images, gold nanoparticles modified with cysteine SAM, are randomly distributed on the surface, possessing a dendritic shape and non-homogenous size. In comparison, gold nanoparticles modified with cysteine SAM and further modified with SDS are homogenously distributed on the surface, better dispersed and highly packed. The interaction between the anionic SDS and cationic cysteine SAM allows the reorganization and redispersion of gold nanoparticles. A spongy film was observed in Fig. 11(B) which may be due to the surfactant film on the surface.

Atomic force microscopy is a powerful tool to measure topography and properties of surfaces. The AFM technique was employed to illustrate the self-assembly process of Au-Au_{nano}-Cys-SDS electrode. Fig. 11(C) shows the AFM 3D image of Au-Au_{nano}-Cys-SDS electrode by the contact mode. Typical AFM 3D images of bare Au, Au-Au_{nano}, and Au-Au_{nano}-Cys-SDS electrodes by the non-contact mode were taken (figures not shown).

4. Conclusions

In this work, the difference in the electrochemical behavior of SAMs of cysteine at Au and Au-Au_{nano} are compared for the first time. In this study, the selective and simultaneous determination of tertiary mixture of AA, DA, and APAP using Au-Au_{nano}-Cys electrode in presence of SDS has been demonstrated. A novel approach for the utilization of anionic surfactants in electroanalytical applications has been described in this work. The negatively charged SDS

adsorbed onto the electrode surface control the electrode reactions of AA, DA, and APAP that differ in their net charge. The negative charge of the adsorbed surfactant film as well as the hydrophobic character of the interior of this film will act to repel hydrophilic AA molecules or its AA^- (if it is present) away from the electrode surface while enhancing the preconcentration/accumulation of hydrophobic cations of DA and APAP. Au-Au_{nano}-Cys electrode in presence of SDS provides better stability to repeated cycles and demonstrates long term stability due to the formation of the strong Au—S bond. Very small peak separation, almost zero or 15 mV peak separation (almost zero or 15 mV peak separation) is obtained indicating unusual high reversibility to repeated cycles. The modified electrode showed high reproducibility, sensitivity, and better stability, not only for DA detection (one component), but also, for tertiary mixture separation.

Acknowledgment

The authors would like to acknowledge the financial support from Cairo University through the Vice President Office for Research Funds.

Appendix A. Supplementary data

Supplementary data associated with this article can be found, in the online version, at doi:10.1016/j.talanta.2012.02.032.

References

[1] N.F. Atta, M.F. El-Kady, A. Galal, Anal. Biochem. 400 (2010) 78.
[2] N.F. Atta, M.F. El-Kady, Sens. Actuators B 145 (2010) 299.
[3] N.F. Atta, M.F. El-Kady, A. Galal, Sens. Actuators B 141 (2009) 566.
[4] N.F. Atta, M.F. El-Kady, Talanta 79 (2009) 639.
[5] N.F. Atta, A. Galal, R.A. Ahmed, Bioelectrochemistry 80 (2011) 132.
[6] N.F. Atta, A. Galal, F.M. Abu-Attia, S.M. Azab, J. Electrochem. Soc. 157 (9) (2010) F116.
[7] G.-Z. Hu, D.-P. Zhang, W.-L. Wu, Z.-S. Yang, Colloids Surf. B 62 (2008) 199.
[8] R.N. Goyal, V.K. Gupta, M. Oyama, N. Bachheti, Talanta 72 (2007) 976.
[9] R.N. Goyal, A. Aliumar, M. Oyama, J. Electroanal. Chem. 631 (2009) 58.
[10] C. Zanardi, F. Terzi, R. Seeber, Sens. Actuators B 148 (2010) 277.
[11] S. Thiagarajan, S.-M. Chen, Talanta 74 (2007) 212.
[12] J. Li, X. Lin, Sens. Actuators B 124 (2007) 486.
[13] Y. Chen, L.-R. Guo, W. Chen, X.-J. Yang, B. Jin, L.-M. Zheng, X.-H. Xia, Bioelectrochemistry 75 (2009) 26.
[14] Q. Bin, Y.X. Rong, Chin. J. Anal. Chem. 35 (2) (2007) 196.
[15] H. Wackerbarth, M. Grubb, J. Wengel, I. Chorkendorff, J. Ulstrup, Surf. Sci. 600 (2006) L122.
[16] L. jiang, A. Glidle, C.J. McNeil, J.M. Cooper, Biosens. Bioelectron. 12 (1997) 1143.
[17] K.I. Ozoemena, T. Nyokong, Electrochim. Acta 51 (2006) 2669.
[18] R.K. Shervedani, M. Bagherzadeh, S.A. Mozaffari, Sens. Actuators B 115 (2006) 614.
[19] X.-H. Zhang, S.-F. Wang, Sens. Actuators B 104 (2005) 29.
[20] H.F. Arlinghaus, M. Schröder, J.C. Feldner, O. Brandt, J.D. Hoheisel, D. Lipinsky, Appl. Surf. Sci. 231 (2004) 392.
[21] Q. Wang, N. Jiang, N. Li, Microchem. J. 68 (2001) 77.
[22] H.-M. Zhang, N.-Q. Li, Z. Zhu, Microchem. J. 64 (2000) 277.
[23] Y.Q. Zhao, H.Q. Luo, N.B. Li, Sens. Actuators B 137 (2009) 722.
[24] M. Wang, C. Sun, L. Wang, X. Ji, Y. Bai, T. Li, J. Li, J. Pharm. Biomed. Anal. 33 (2003) 1117.
[25] Y.-S. Chen, J.-H. Huang, Diamond Relat. Mater. 18 (2009) 516.
[26] C.R. Raj, S. Behera, J. Electroanal. Chem. 581 (2005) 61.
[27] M. Klis, E. Maicka, A. Michota, J. Bukowska, S. Sek, J. Rogalski, R. Bilewicz, Electrochim. Acta 52 (2007) 5591.
[28] Y. Saga, H. Tamiaki, J. Photochem. Photobiol. B 73 (2004) 29.
[29] J. Li, G. Cheng, S. Dong, Thin Solid Films 293 (1997) 200.
[30] A.-S. Duwez, J. Electron Spectrosc. Relat. Phenom. 134 (2004) 97.
[31] P. Maksymovych, O. Voznyy, D.B. Dougherty, D.C. Sorescu, J.T. Yates Jr., Prog. Surf. Sci. 85 (2010) 206.
[32] L.-J. Fan, Y.-W. Yang, Y.-T. Tao, J. Electron Spectrosc. Relat. Phenom. 144 (2005) 433.
[33] C.R. Raj, T. Okajima, T. Ohsaka, J. Electroanal. Chem. 543 (2003) 127.
[34] L. Su, L. Mao, Talanta 70 (2006) 68.
[35] L. Zhang, R. Yuan, Y. Chai, X. Li, Anal. Chim. Acta 596 (2007) 99.
[36] Y. Xian, H. Wang, Y. Zhou, D. Pan, F. Liu, L. Jin, Electrochem. Commun. 6 (2004) 1270.
[37] J.-D. Qiu, M. Xiong, R.-P. Liang, H.-P. Peng, F. Liu, Biosens. Bioelectron. 24 (2009) 2649.
[38] E. Briand, M. Salmain, C. Comp'ere, C.-M. Pradier, Colloids Surf. B 53 (2006) 215.
[39] B. Arezki, A. Delcorte, P. Bertrand, Appl. Surf. Sci. 231 (2004) 122.
[40] S. Wang, D. Du, Sensors 2 (2002) 41.
[41] M.J. Giz, B. Duong, N.J. Tao, J. Electroanal. Chem. 465 (1999) 72.
[42] G. Hager, A.G. Brolo, J. Electroanal. Chem. 550 (2003) 291.
[43] S.K. Moccelini, S.C. Fernandes, I.C. Vieira, Sens. Actuators B 133 (2008) 364.
[44] W. Yang, J.J. Gooding, D.B. Hibbert, J. Electroanal. Chem. 516 (2001) 10.
[45] L.L. Jun, Y.L. Bo, C.Q. Feng, C. Hao, W.F. Min, W.J. Ling, K.H. Xing, Chin. J. Anal. Chem. 35 (7) (2007) 933.
[46] J.-J. Feng, G. Zhao, J.-J. Xu, H.-Y. Chen, Anal. Biochem. 342 (2005) 280.
[47] Y.-C. Liu, S.-Q. Cui, J. Zhao, Z.-S. Yang, Bioelectrochemistry 70 (2007) 416.
[48] S.-f. Wang, D. Du, Q.-C. Zou, Talanta 57 (2002) 687.
[49] Y. Zhuo, R. Yu, R. Yuan, Y. Chai, C. Hong, J. Electroanal. Chem. 628 (2009) 90.
[50] G. Dodero, L. De Michieli, O. Cavalleri, R. Rolandi, L. Oliveri, A. Dacca, R. Parodi, Colloids Surf. A 175 (2000) 121.
[51] M.S. El-Deab, T. Ohsaka, Electrochem. Commun. 5 (2003) 214.
[52] A. Kühnle, Curr Opin, Colloid Interface Sci. 14 (2009) 157.
[53] Y. Zhao1, J. Bai1, L. Wang, X.E.P. Huang, H. Wang, L. Zhang, Int. J. Int. J. Electrochem. Sci. 1 (2006) 363.
[54] S. Aryal, K.C. Remant Bahadur, N. Dharmaraj, N. Bhattarai, C.H. Kim, H.Y. Kim, Spectrochim. Acta A 63 (2006) 160.
[55] W. Qian, J.-H. Zhuang, Y.-H. Wang, Z.-X. Huang, J. Electroanal. Chem. 447 (1998) 187.
[56] T. Łuczak, Electrochim. Acta 54 (2009) 5863.
[57] N.F. Atta, A. Galal, F.M.A. Attia, S.M. Azab, Electrochim. Acta 56 (2011) 2510.
[58] N.F. Atta, S.A. Darwish, S.E. Khalil, A. Galal, Talanta 72 (2007) 1438.
[59] C. Li, Y. Ya, G. Zhan, Colloids Surf. B 76 (2010) 340.
[60] I.F. Ramos, M.C. Acevedo, M.A. Scibioh, C.R. Cabrera, J. Electroanal. Chem. 650 (2010) 98.